



Hydrothermal synthesis of magnetic CoFe_2O_4 nanoparticles and $\text{CoFe}_2\text{O}_4/\text{MWCNTs}$ nanocomposites for U and Pb removal from aqueous solutions

Z. Rahimi¹ · H. Sarafraz¹ · Gh. Alahyarizadeh¹  · A. S. Shirani¹

Received: 12 February 2018 / Published online: 5 May 2018
© Akadémiai Kiadó, Budapest, Hungary 2018

Abstract

Magnetite CoFe_2O_4 nanoparticle and $\text{CoFe}_2\text{O}_4/\text{MWCNT}$ nanocomposite adsorbents with high specific surface area, high adsorption capacity, and easily separable property were synthesized by the hydrothermal method for uranium and lead removal from aqueous solutions. The synthesized samples were characterized by FT-IR, XRD, SEM, and BET analysis. The estimated specific surface areas were obtained as 113.4 and 186.1 $\text{m}^2 \text{g}^{-1}$ for CoFe_2O_4 and $\text{CoFe}_2\text{O}_4/\text{MWCNTs}$, respectively. The synthesized nanostructures resulted in achieving the maximum monolayer adsorption capacity. The adsorption capacity of U(VI) and Pb(II) onto CoFe_2O_4 nanoparticles and $\text{CoFe}_2\text{O}_4/\text{MWCNT}$ nanocomposites were obtained as 294.12 (at pH 5) and 500 mg g^{-1} (at pH 6) for uranium and 109.89 and 217.39 mg g^{-1} for lead (at pH 5), respectively, which indicated the favorable effects of decorated MWCNT on the removal of uranium and lead. Several parameters, including pH, contact time, initial U(VI) concentration and solution volume, and adsorbent concentration, which influence the adsorption capacity, were also investigated.

Keywords Magnetic CoFe_2O_4 nanoparticle · Magnetic $\text{CoFe}_2\text{O}_4/\text{MWCNT}$ nanocomposite · Hydrothermal synthesis · Uranium and lead adsorption

Introduction

A serious worldwide environmental problem caused by toxic and radioactive heavy metals, such as Cu, Cd, As, Pb, and U, is water and soil pollution. These dangerous materials have significant impacts on the environment and consequently human health [1–3]. Uranium is a toxic and radioactive substance that usually exists in hexavalent oxidation state. It can naturally be found in subsurface environments and as industrial waste in the nuclear facilities and phosphate-based fertilizer companies [4, 5]. Living organisms are directly destroyed by uranium when it enters the body by mistake through any kinds of radioactive sources, such as dust in the air and particle in water and soil. Inside the body, uranium generates reactive radicals

that consequently react with bio-molecules and causes several detrimental diseases, including liver and kidney damage, and even death [6, 7]. The maximum value of uranium in the drinking water is 2 $\mu\text{g/l}$, as designated by the World Health Organization (WHO) [8]. Lead is another heavy metal that is considered as the most harmful metal ion to the environment. It seriously influences the central nervous system. Similar to uranium, lead causes harm to the liver and reproductive system, kidney, basic cellular processes, and brain functions [9]. The upper limit of lead in the drinking water is 0.05 mg/l , as designated by WHO [10].

Several techniques, such as chemical precipitation, solvent extraction, ion exchange, electrolysis, membrane separation, activated sludge, reverse osmosis, flocculation (coagulation), and adsorption, are used for water treatment. They differ in their degree of success to remove heavy metals and treat wastewaters [11–15]. Adsorption method is considered as one of the most famous and widespread among the above mentioned treatment techniques due to its various advantages, such as environmental friendliness,

✉ Gh. Alahyarizadeh
g_alahyarizadeh@yahoo.com

¹ Engineering Department, Shahid Beheshti University, G.C., P.O. Box 1983969411, Tehran, Iran

wide adaptability, low cost, convenient operation, and high efficiency [16, 17]. Adsorbent properties, including specific surface area and particle sizes, are the essential factors that affect the adsorption efficiency. Therefore, synthesizing and developing an effective adsorbent is significant in the water treatment applications [18].

The magnetic nanoparticles due to several advantages such as the feasibility of preparation, easy separation (by an external magnetic field), high surface areas, and high chemical and mechanical stability attract increasing attention as potential adsorbents for heavy metal removal from aqueous solutions [19–22]. In the past decades, various magnetic materials, including a type of ferrites, $M^{II}Fe_2O_4$ ($M = Co, Zn, Mg, Cu, \text{etc.}$), have been widely used in different technological applications [23]. Among the possible ferrite materials, $CoFe_2O_4$ is an interesting candidate for adsorption applications due to moderate saturation magnetization, exceptional chemical stability, and adequate mechanical hardness [24]. The nanostructured magnetic materials are synthesized by several methods, such as thermal decomposition of organometallic compounds, sol-gel method, co-precipitation, and hydrothermal synthesis [25–29]. Hydrothermal, which is also called solvothermal method, is the well-established method that is widely used to synthesize many nanoparticle materials. The kinetics of this method is typically slow due to relatively low temperatures of the synthesis process [30]. To enhance the specific surface area and adsorption capacity, the magnetic nanoparticles were coated by several materials or coated on various materials, including polyacrylamide [29], ethylenediamine tetraacetate (EDTA) [25], silica [31], graphene oxide [18], and carbon nanotubes (CNT) [22].

Recently, multi-wall carbon nanotubes (MWCNTs) have been widely used in various industries because of their unique structures and properties. MWCNTs present large surface areas, rich surface chemical functionalities, high aspect ratios, and nano-sized stability. Their usage has been widely spread in chemistry, catalysis, and nanoelectronic and magnetic devices [32]. Moreover, MWCNTs have been considered as a new adsorbent or as an additive to the adsorbents to increase total specific surface area and consequently adsorption capacity for immobilization of radiative and poisonous heavy metal and organic/inorganic contaminants [33–35]. However, MWCNTs are very hydrophobic. They easily aggregate in aqueous solution due to the high van der Waals interaction forces between MWCNTs, which cause effectively slowing down of adsorption behaviors and consequently reducing the adsorption capacity [36]. Therefore, combining the advantages of MWCNTs and magnetic nanoparticles with decoration of MWCNTs by $CoFe_2O_4$ can produce a potential novel adsorbent with enhanced specific surface

area, desirable absorptivity, and effective magnetic separability [18].

Shen et al. synthesized the magnetite Fe_3O_4 nanoparticles with different average sizes by the co-precipitation method to remove different heavy metal ions, including Cd^{2+} , Cr^{6+} , Cu^{2+} , and Ni^{2+} from wastewater; $FeCl_3$ and $FeCl_2$ were used as Fe sources to synthesize magnetic nanoparticles. They could achieve the different particle sizes of 8–35 nm magnetic Fe_3O_4 nanoparticles [37]. Habibi et al. synthesized the $CoFe_2O_4$ nanoparticles by wet chemical route. They used $CoCl_2$ and $FeCl_3$ as the magnetic element sources. The $CoFe_2O_4$ nanoparticles sizes of 47 nm were achieved [38]. Zhang et al. synthesized and characterized the bimetal oxide magnetic nanoparticles ($MnFe_2O_4$ and $CoFe_2O_4$) through the chemical co-precipitation method using $FeCl_3$, $Mn(NO_3)_2$, and $Co(NO_3)_2$. They investigated the adsorption capacity of arsenic compounds on $MnFe_2O_4$ and $CoFe_2O_4$ nanoparticles and compared with Fe_3O_4 . They observed that the maximum adsorption capacities for arsenite and arsenate were 94 and 90 $mg\ g^{-1}$ and 100 and 74 $mg\ g^{-1}$ for $MnFe_2O_4$ and $CoFe_2O_4$, respectively, which were higher than those for Fe_3O_4 [39]. Olmos et al. prepared different MFe_2O_4 nanoferrites ($M = Co, Ni, \text{and Zn}$) through the mechanochemical method and using $FeCl_3$ and MCl_2 to study the adsorption of $Pb(II)$ from aqueous solution. They found a maximum adsorption capacity of 20.58 mg/g for $CoFe_2O_4$ [40]. Wei et al. investigated the adsorption capacity of $CoFe_2O_4$ to remove uranium from aqueous solutions. They reported a maximum adsorption capacity of 170.07 mg/g [41]. Fafous et al. investigated uranium (VI) removal from aqueous solutions through MWCNTs. The maximum sorption capacity reported for uranium (VI) ions was 39.5 $mg\ g^{-1}$ [42]. Liu et al. decorated the magnetic ferrite nanoparticles of MFe_2O_4 ($M = Fe, Co, Ni$) on CNTs through in situ high-temperature hydrolysis and polymerizing of metal chlorides, including $FeCl_3$, $CoCl_2$, and CNTs in polyol solution [43]. The synthesis of $CoFe_2O_4/CNT$ magnetic nanocomposites was also reported by Jiang et al. They synthesized the $CoFe_2O_4/CNT$ magnetic nanocomposites through a solvothermal treatment in ethylene glycol. They used a mixture of metal chlorides, including $FeCl_3$ and $CoCl_2$, sodium acetate, polyethylene glycol, and MWCNTs [44]. Tan et al. investigated the adsorption capacity of uranium (VI) on the synthesized $CoFe_2O_4$ and $CoFe_2O_4/MWCNTs$. They used a hydrothermal method using $FeSO_4 \cdot 7H_2O$ and $CoCl_2 \cdot 4H_2O$ to synthesize the magnetic nanoparticles and nanocomposites. The reported maximum adsorption capacity for uranium (VI) based on Langmuir model was 212.7 mg/g for $CoFe_2O_4/MWCNTs$, which indicated a high efficiency of uranium removal from aqueous solutions [22]. Zhu et al. synthesized functionalized magnetic mesoporous silica by solvothermal treatment

to remove uranium from aqueous solutions. They decorated the magnetite Fe_3O_4 nanoparticles to reach higher uranium adsorption by synthesizing two new adsorbents of $\text{Fe}_3\text{O}_4@n\text{SiO}_2@m\text{SiO}_2$ and $\text{Fe}_3\text{O}_4@n\text{SiO}_2@m\text{SiO}_2\text{-DIM}$ [53]. In another research, Guo et al. synthesized functionalized magnetic $\text{Fe}_3\text{O}_4@n\text{SiO}_2$ by simply embedding iron oxide into MCM-41. They reported large sorption capacity of 160 mg/g [54]. Table 1 summarizes the main parameters in the above-listed literature reviews including the synthesized adsorbents, the preparation method, the important chimerical materials which were used in the synthesis procedure, and their applications.

In the present study, magnetite CoFe_2O_4 nanoparticles and $\text{CoFe}_2\text{O}_4/\text{MWCNTs}$ nanocomposites were synthesized by hydrothermal method. The synthesized samples were characterized by different characterization analyses, including Fourier transform infrared spectroscopy (FT-IR), X-ray diffraction (XRD), scanning electron microscopy (SEM), and Brunauer–Emmett–Teller (BET) method. The adsorption properties of prepared CoFe_2O_4 nanoparticles and $\text{CoFe}_2\text{O}_4/\text{MWCNTs}$ nanocomposites were also investigated by applying them as sorbents to sorb U(VI) and Pb(II) ions from wastewater. The batch sorption technique was used to assess the adsorbability of magnetite CoFe_2O_4 nanoparticles from the wastewater. Several parameters including pH, contact time, initial U(VI) concentration and solution volume, and adsorbent concentration, which influence the adsorption capacity, were also investigated.

Experimental section

Chemicals

The iron source, cobalt source, sodium source, and solvent that were used in this study are $\text{FeCl}_3 \cdot 6\text{H}_2\text{O}$, $\text{CoCl}_2 \cdot 6\text{H}_2\text{O}$, sodium carbonate (Na_2CO_3), and ethylene glycol. To investigate adsorption, 1000 ppm uranium standard ($\text{UO}_2(\text{NO}_3)_2$) and lead standard ($\text{Pb}(\text{NO}_3)_2$) were also used to prepare sample solutions. All chemicals were purchased from Merck Co. The MWCNTs that were used in this work have the specifications including diameters of 10–20 nm and purity of 95–98%. To adjust the solution pH, negligible volumes of sodium hydroxide solution were used.

Preparation of CoFe_2O_4 nanoparticles

CoFe_2O_4 nanoparticles were prepared by a multistep hydrothermal method. At first, 3 g of $\text{FeCl}_3 \cdot 6\text{H}_2\text{O}$ and 1.32 g of $\text{CoCl}_2 \cdot 6\text{H}_2\text{O}$ were dissolved in 10 ml ethylene glycol. After that, 2.35 g of sodium carbonate (Na_2CO_3) was added to the mixture with stirring for about 30 min to 60 min. Then, the resulting solution was poured into a Teflon-lined autoclave with a stainless-steel cover and heated to 200 °C for 24 h. The final products were cooled to room temperature. The black precipitate was collected by a magnet, washed with distilled water and ethanol repeatedly to remove the impurities and dried at 70 °C in a vacuum oven for 6 h.

Table 1 The list of main parameters in synthesis and application of the investigated adsorbents in the literature reviews

Adsorbents	Preparation method	Chemical materials used for preparation	Removal heavy metal by synthesized adsorption	References
Fe_3O_4	Co-precipitation	FeCl_3 and FeCl_2	Cd^{2+} , Cr^{6+} , Cu^{2+} , and Ni^{2+}	[37]
CoFe_2O_4	Wet chemical route	CoCl_2 and FeCl_3	–	[38]
MnFe_2O_4 and CoFe_2O_4	Co-precipitation	FeCl_3 , $\text{Mn}(\text{NO}_3)_2$, and $\text{Co}(\text{NO}_3)_2$	As	[39]
MFe_2O_4 (M = Co, Ni, and Zn)	Mechanochemical	FeCl_3 and MCl_2	Pb(II)	[40]
CoFe_2O_4	Solvothermal	$\text{FeSO}_4 \cdot 7\text{H}_2\text{O}$ and $\text{CoCl}_2 \cdot 4\text{H}_2\text{O}$	U(VI)	[41]
MWCNTs	–	–	U(VI)	[42]
MFe_2O_4 (M = Fe, Co, Ni) on CNTs	Hydrolysis and polymerizing	FeCl_3 , CoCl_2 , and CNTs	–	[43]
$\text{CoFe}_2\text{O}_4/\text{CNT}$	Solvothermal	FeCl_3 and CoCl_2	–	[44]
CoFe_2O_4 and $\text{CoFe}_2\text{O}_4/\text{MWCNTs}$	Hydrothermal	$\text{FeSO}_4 \cdot 7\text{H}_2\text{O}$ and $\text{CoCl}_2 \cdot 4\text{H}_2\text{O}$	U(VI)	[22]
Fe_3O_4 and $\text{Fe}_3\text{O}_4@n\text{SiO}_2@m\text{SiO}_2$	Solvothermal	$\text{FeCl}_3 \cdot 6\text{H}_2\text{O}$ TEOS, and CTAB	U(VI)	[53]
$\text{Fe}_3\text{O}_4@n\text{SiO}_2$	Co-condensation	$\text{FeCl}_3 \cdot 6\text{H}_2\text{O}$ TEOS, CTAB and APS	U(VI)	[54]

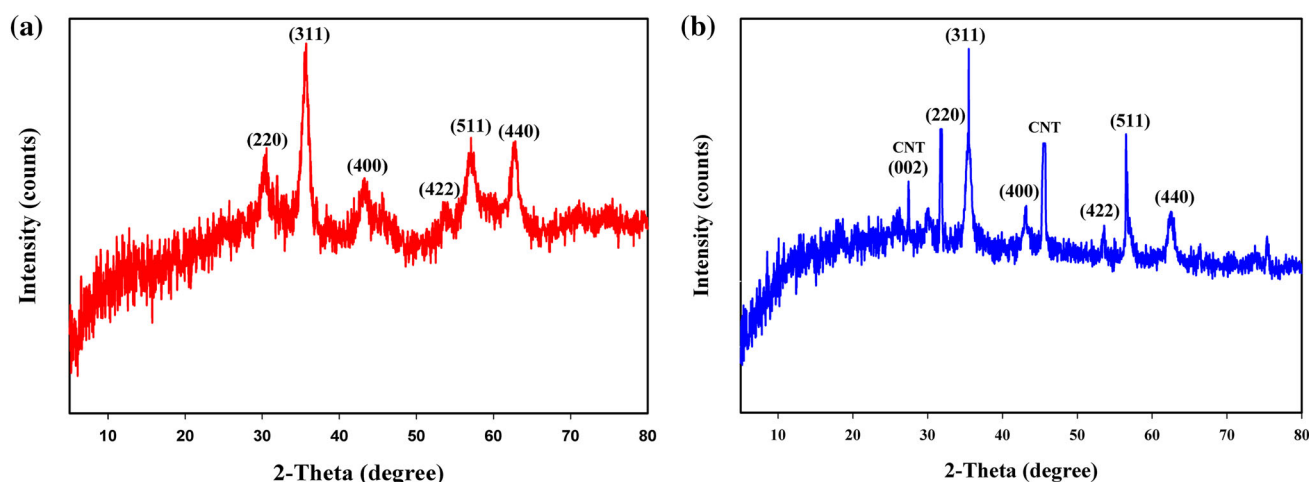


Fig. 1 Powder X-ray diffraction (XRD) patterns of magnetite **a** CoFe_2O_4 nanoparticles, **b** $\text{CoFe}_2\text{O}_4/\text{MWCNTs}$ nanocomposite

Preparation of $\text{CoFe}_2\text{O}_4/\text{MWCNTs}$ nanocomposites

For the decoration of MWCNTs, an appropriate amount of MWCNTs was dispersed in 40 ml ethylene glycol by sonication for 30 min. Then, 3 g of $\text{FeCl}_3 \cdot 6\text{H}_2\text{O}$, 1.32 g of $\text{CoCl}_2 \cdot 6\text{H}_2\text{O}$, and 2.35 g of sodium carbonate (Na_2CO_3) were added to the prepared mixture with sonication for approximately 30 min to 60 min. Furthermore, similar reaction conditions that were used for the synthesis of CoFe_2O_4 nanoparticles were used to produce $\text{CoFe}_2\text{O}_4/\text{MWCNTs}$ nanocomposites.

Characterization

The magnetic CoFe_2O_4 nanoparticles and $\text{CoFe}_2\text{O}_4/\text{MWCNTs}$ nanocomposites were characterized by XRD, scanning electron microscopy (SEM), energy-dispersive X-ray spectrometry (EDS), FTIR spectroscopy, and Brunauer–Emmett–Teller (BET) method. XRD (Bruker D8 Advance) was used to collect XRD patterns at 30 kV and 20 mA and $\text{Cu K}\alpha$ radiation ($\lambda = 0.1540598$ nm). A TENSOR 27 FTIR spectrometer was used to record FTIR spectra of synthesized samples. The morphology and particle sizes of synthesized MSs were measured using FE-SEM (ZEISS- SIGMA-VP-500). The BET surface area and pore size distributions were obtained from the nitrogen adsorption–desorption isotherms obtained by BELSORP-mini analyzers (BEL Japan, Inc.). The element concentrations in adsorption experiments were analyzed by SPECTRO Genesis simultaneous CCD-based radially viewed ICP-OES.

Adsorption tests

Adsorption experiments were performed by adding different amounts of CoFe_2O_4 or $\text{CoFe}_2\text{O}_4/\text{MWCNTs}$ in uranium

or lead solution at various conditions, including different solution concentrations, volumes and pH values, and contact times. After the treatment, solid phase was separated from the solution by using a magnet. The initial and equilibrium concentrations of uranium or lead were determined using ICP-OES. Standard and sample solutions were prepared from 1000 ppm uranium standard ($\text{UO}_2(\text{NO}_3)_2$) and lead standard ($\text{Pb}(\text{NO}_3)_2$). Analytical calibration curves for U and Pb were obtained from 0.0, 1.0, 5.0, 10.0, 25.0, 50.0 and 100.0 ppm by diluting of 1000 ppm standard solutions. The measurement range for both samples were 0.8 ppm – 110 ppm with 0.9999 correlation coefficient for U and 0.9997 for Pb. High intensity emission and recommended lines of uranium and lead by ICP-OES apparatus were selected to determine the uranium concentration. The U(VI) or Pb(II) removal percentage (%) and the adsorption capacity (Q_e , mg/g) were calculated using the following equations [1]:

$$\text{Adsorption capacity (mg/g)} = \frac{(C_i - C_f) \times V}{m} \quad (1)$$

$$\text{Removal (\%)} = \frac{(C_i - C_f) \times 100}{C_i} \quad (2)$$

where C_i is the initial concentration and C_f is the concentration at equilibrium after treatment; m (mg) and V (ml) are the mass of the adsorbent and the volume of the solution, respectively.

Results and discussion

The phase structures of the synthesized CoFe_2O_4 nanoparticles and $\text{CoFe}_2\text{O}_4/\text{MWCNTs}$ nanocomposites are shown in Fig. 1. As shown in Fig. 1a, the XRD pattern of the synthesized magnetite CoFe_2O_4 nanoparticles indicates the presence of the characteristic peaks of (220), (311),

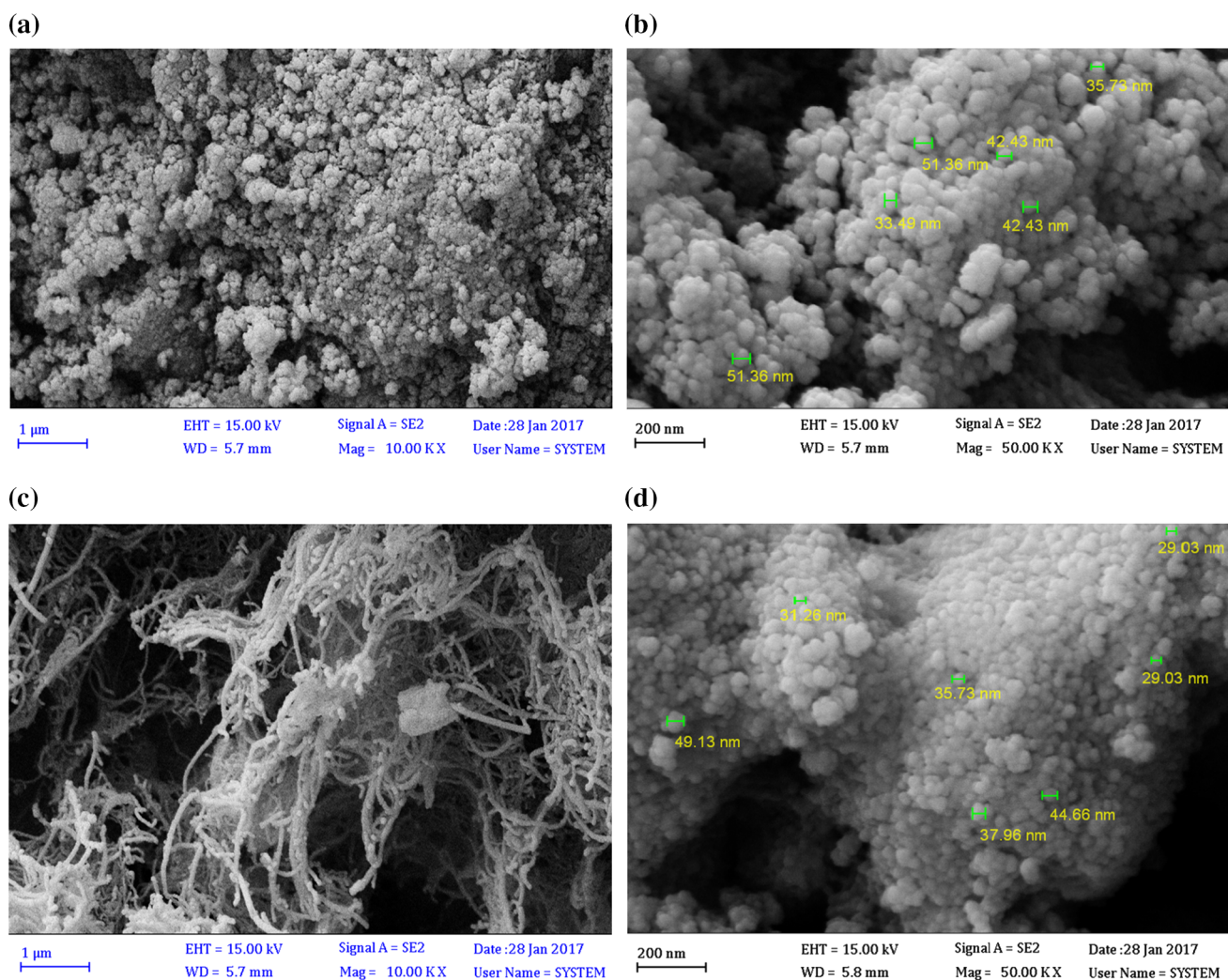


Fig. 2 The SEM images of the synthesized magnetic **a, b** CoFe_2O_4 nanoparticles, **c, d** $\text{CoFe}_2\text{O}_4/\text{MWCNTs}$ nanocomposite

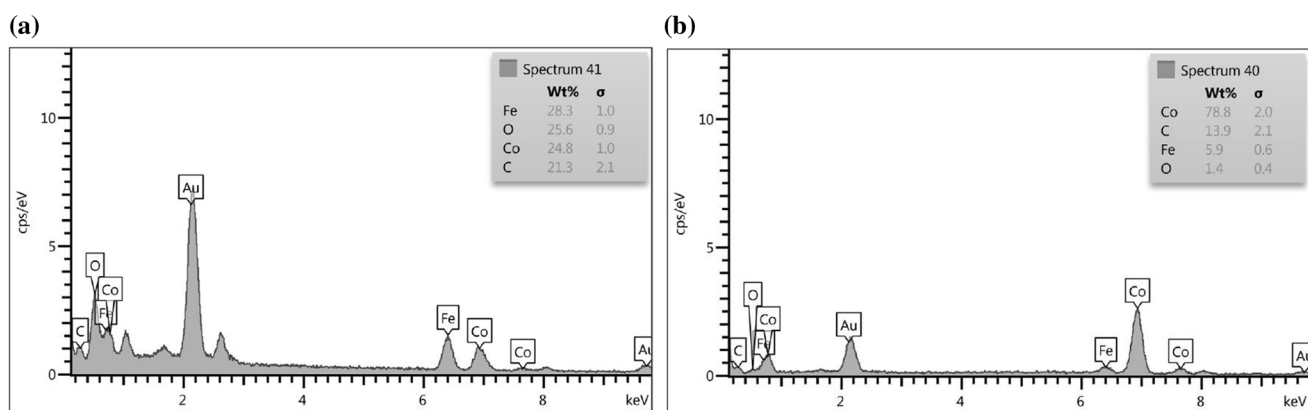


Fig. 3 EDS diagram of **a** CoFe_2O_4 , **b** $\text{CoFe}_2\text{O}_4/\text{MWCNTs}$ nanostructures for one point of their surfaces

(400), (422), (511), and (440), which were observed at the diffraction angles of $2\theta = 30.23, 35.69, 43.26, 53.99, 57.29,$ and 62.83 , respectively. These peaks are the main

characteristic peaks of CoFe_2O_4 , which confirm that the resultant nanoparticles are pure CoFe_2O_4 . As can be observed, the position and intensities of nearly all of the

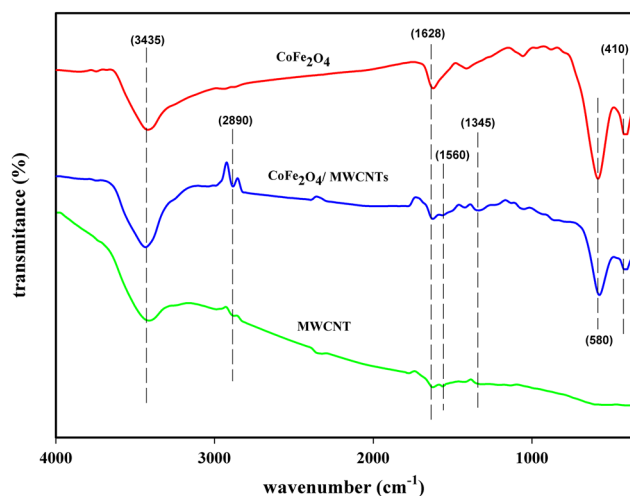


Fig. 4 Fourier transform infrared (FT-IR) spectra of MWCNTs, magnetite CoFe_2O_4 nanoparticles and $\text{CoFe}_2\text{O}_4/\text{MWCNTs}$ nanocomposites

peaks are well matched to those of the other experimental results and the standard PDF cards for CoFe_2O_4 nanoparticles (JCPDS 22-1086 and JCPDS 79-1744) [16, 45, 46]. Figure 1b shows the XRD pattern of the synthesized $\text{CoFe}_2\text{O}_4/\text{MWCNTs}$ nanocomposites. The additional peak (002) that could be observed at 27.5° corresponds to graphite because of adding MWCNTs to the structure. As shown in this figure, the characteristic peaks related to the CoFe_2O_4 nanoparticles, which are decorated on the MWCNTs, are approximately same as before, and a few peaks related to the MWCNTs were added to the XRD pattern [16].

The microstructures of the synthesized magnetic CoFe_2O_4 nanoparticles and $\text{CoFe}_2\text{O}_4/\text{MWCNTs}$ nanocomposites were also characterized by SEM. The SEM images of synthesized magnetic nanoparticles, which are shown in Fig. 2a and b, indicate that the synthesized magnetic CoFe_2O_4 nanoparticles are composed of spherical nanoparticles that have the average diameter of approximately 40 nm. The SEM images of magnetic $\text{CoFe}_2\text{O}_4/\text{MWCNTs}$ nanocomposites, which are shown in Fig. 2c and d, also indicate that the average diameter of CoFe_2O_4 nanoparticles decorated on MWCNTs is approximately 34 nm. The EDS spectra of the synthesized CoFe_2O_4 and $\text{CoFe}_2\text{O}_4/\text{MWCNTs}$ nanostructures are shown in Fig. 3a and b. The elements of C, Fe, Co, and O can be observed in CoFe_2O_4 and $\text{CoFe}_2\text{O}_4/\text{MWCNTs}$.

Figure 4 shows the FT-IR spectra of MWCNTs, synthesized magnetite CoFe_2O_4 nanoparticles, and $\text{CoFe}_2\text{O}_4/\text{MWCNTs}$ nanocomposites. As shown in this figure, the IR spectra of different nanostructures include several main absorption bands. The absorption bands, which are located at about 580 and 410 cm^{-1} , are related to the stretching

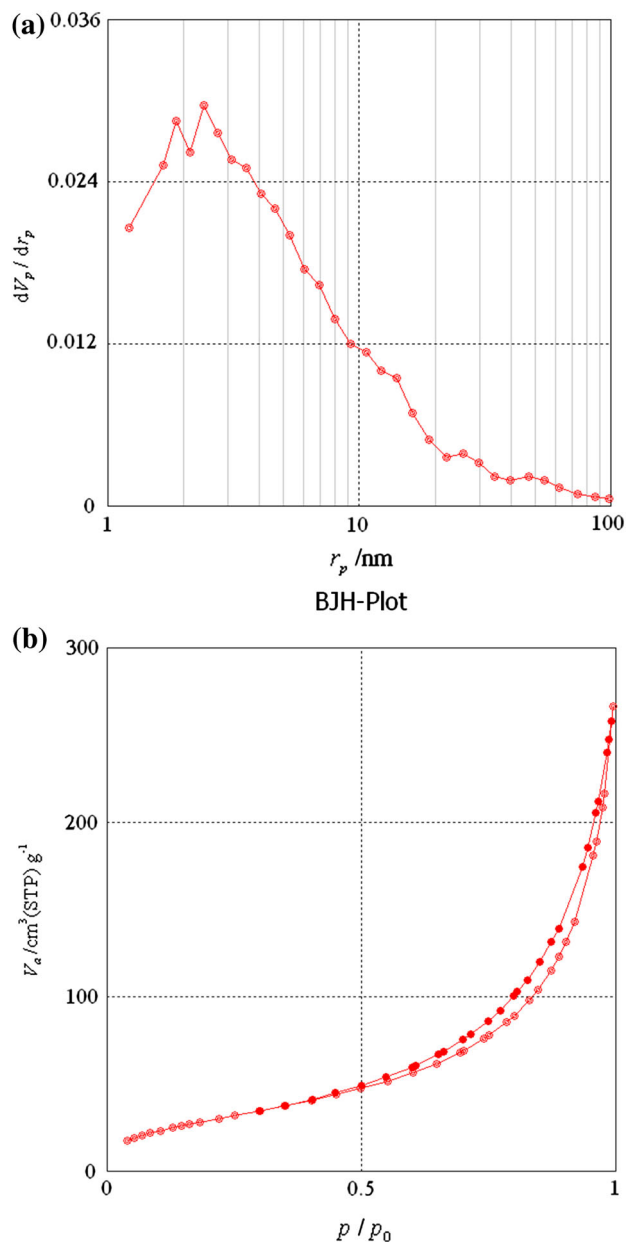


Fig. 5 N_2 adsorption–desorption isotherms measured 76 K of **a** CoFe_2O_4 and **b** $\text{CoFe}_2\text{O}_4/\text{MWCNTs}$ magnetic material. Inset: pore size distributions from the adsorption branches through the BJH method

vibrations of metal oxide in octahedral group complex Co(II)-O^{2-} and Fe(III)-O^{2-} tetrahedral group. These tetrahedral groups mainly confirm the existence of spinel ferrite and complex of the cobalt ferrite in the synthesized nanostructures [47, 48]. The absorption peak at around 1628 cm^{-1} and a broad absorption band near 3435 cm^{-1} are related to the deformation vibrations of adsorbed H_2O molecules and stretching vibrations of OH on the surface of particles [47]. The specific characteristic bands at 2890, 1560, and 1345 cm^{-1} , which are displayed in MWCNT

Table 2 Summary of physical properties of CoFe₂O₄ and CoFe₂O₄/MWCNTs reported previously and those investigated in the present work

sample	Preparation condition	Iron source/cobalt source	Surface area (m ² g ⁻¹)	Pore volume (cm ³ g ⁻¹)	Average pore diameter (nm)	References
CoFe ₂ O ₄	Hydrothermal method	FeSO ₄ ·7H ₂ O/	82.23	0.236	22.96	[22]
CoFe ₂ O ₄ /MWCNTs		CoCl ₂ ·4H ₂ O	170.3	0.441	20.74	
CoFe ₂ O ₄	Hydrothermal precipitation	Fe(NO ₃) ₃ ·9H ₂ O/ Co(NO ₃) ₂ ·6H ₂ O	109.54	0.0505	18.96	[16]
CoFe ₂ O ₄ -NH ₂	Polyol method	Fe(acac) ₃ /CoCl ₂ ·6H ₂ O	136.7	0.63	18.5	[51]
CoFe ₂ O ₄ /MWCNTs-NH ₂			157.5	0.87	22.30	
CoFe ₂ O ₄ -rGO	–	Fe(NO ₃) ₃ ·9H ₂ O/ Co(NO ₃) ₂ ·6H ₂ O	169.9	0.1490	4.054	[18]
CoFe ₂ O ₄ /CNTs-C	Hydrothermal method	Fe(NO ₃) ₃ ·9H ₂ O/	134.4	–	9.65	[52]
CoFe ₂ O ₄ /CNTs-N		Co(NO ₃) ₂ ·6H ₂ O	132.0	–	10.85	
CoFe ₂ O ₄	Chemical coprecipitation	FeCl ₃ ·6H ₂ O/ Co(NO ₃) ₂ ·6H ₂ O	101	–	–	[39]
CoFe ₂ O ₄	Hydrothermal method	FeCl ₃ ·6H ₂ O/	113.4	0.39	2.41	Present work
CoFe ₂ O ₄ /MWCNTs		CoCl ₂ ·6H ₂ O	186.1	0.94	6.06	

and CoFe₂O₄/MWCNTs spectra, are related to the symmetric and asymmetric stretching of C–H, C=C and COO⁻ of MWCNT contents [7, 49].

The N₂ sorption–desorption isotherm, which determines the specific surface area and pore size distributions, was measured at –196 °C in the interval of relative pressures from 10⁻⁶ to 0.995 using ultrahigh purity nitrogen by BELSORP mini analyzers. The samples were pretreated at 400 °C for 8 h. The surface specific area was calculated by BET method. Barrett–Joyner–Halenda (BJH) method was also used to calculate pore size distribution curve. The pore size was defined as the maximum of the pore size distribution curve. The specific surface areas and pore size distributions of the synthesized magnetic CoFe₂O₄ nanoparticles and CoFe₂O₄/MWCNTs nanocomposites are shown in Fig. 5. As shown in Fig. 5a and b, the adsorption–desorption isotherms indicate type III isotherms accompanied by type H3 hysteresis loop [50]. The specific surface areas were calculated as 113.4 and 186.1 m² g⁻¹ using BET equation for CoFe₂O₄ nanoparticles and CoFe₂O₄/MWCNTs nanocomposites, respectively, which indicated much higher values than those in previous reports (Table 2). Barrett–Joyner–Halenda (BJH) method was also used to calculate pore size distribution curve (inset, Fig. 5). The pore size was defined as the maximum of the pore size distribution curve. As shown inside Fig. 5a and b, synthesized magnetic CoFe₂O₄ nanoparticles showed a pore diameter and volume of 2.41 nm and 0.39 cm³ g⁻¹, respectively. The corresponding values for synthesized magnetic CoFe₂O₄/MWCNTs nanocomposites were

increased to 6.06 nm and 0.94 cm³ g⁻¹, respectively. The considerable note is that the synthesized composites exhibit higher BET surface areas, pore volumes, and pore sizes, which were expected to have efficient influence on the enhancement of the heavy metal adsorption capacity from wastewater pollutants.

Uranium and lead adsorption results of synthesized magnetic CoFe₂O₄ nanoparticles and CoFe₂O₄/MWCNTs nanocomposites in different solution pH are shown in Fig. 6a and b, respectively. The influence of the solution pH on the uranium and lead adsorption capacities was investigated using 0.01 g of CoFe₂O₄ or CoFe₂O₄/MWCNTs for a pH range of 2.0–12.0 and 60 min treatment time. The initial concentrations of uranium and lead solution were 50 ppm in 15 and 50 ml, respectively. As shown in these figures, the solution pH plays a significant role on the sorption behavior of metal ions on CoFe₂O₄ and CoFe₂O₄/MWCNTs. Results showed that the adsorption capacity increases with a pH rise from 2.0 to around 5.0 and decreases with further increase in pH from 5.0 to 12.0. The optimum pH for Pb(II) sorption onto both CoFe₂O₄ and CoFe₂O₄/MWCNTs was obtained around 5, whereas the optimum pH for U(VI) sorption onto CoFe₂O₄ nanoparticles was 6.0 and around 5 onto CoFe₂O₄/MWCNTs nanocomposites. In pH lower than optimum pH, the adsorption process is not favored, because the surface of adsorbent and the adsorbed metal ions are positively charged. Moreover, many adsorption sites were occupied by excess H⁺. By increasing pH higher than optimum pH, anionic species of metal ions become major carriers in the

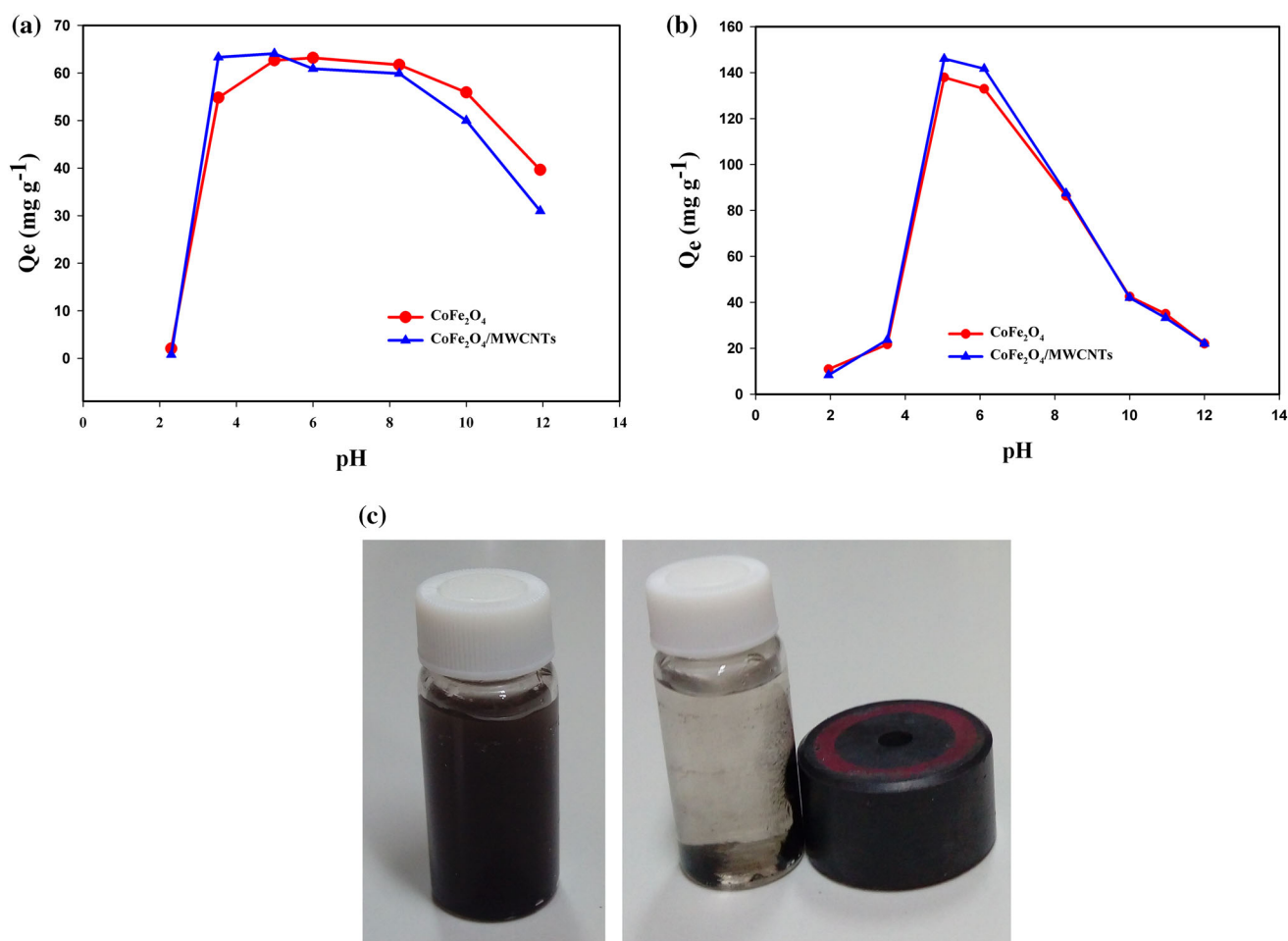


Fig. 6 Effect of solution pH on **a** U(VI) adsorption, **b** Pb(II) adsorption by magnetite CoFe₂O₄ nanoparticles and CoFe₂O₄/MWCNTs nanocomposites, and **c** photographs of CoFe₂O₄ dispersion and magnetic separation

solution, which results in forming hydroxyl dissolved carbonate and bicarbonate anions, such as $\text{UO}_2(\text{CO}_3)_3^{4-}$, $(\text{UO}_2)_2\text{CO}_3(\text{OH})_3^-$, and $\text{UO}_2(\text{OH})_3^-$. These anion complexes lead to a slight decrease in adsorption capacity and removal efficiency. The magnetic property of the synthesized nanostructures adsorbents, which exhibits that they could easily separate from their dispersed solution using a normal magnet, is shown in Fig. 6c.

The adsorption capacities of uranium and lead ions on CoFe₂O₄ and CoFe₂O₄/MWCNTs as a function of treatment time or contact time of 2–90 min for uranium and 2–180 min for lead are shown in Fig. 7a and b, respectively. The initial concentration of U(VI) in the aqueous solution was 35 ppm in 60 ml, and the quantity of synthesized adsorbents was considered to be 0.002 g. The values for Pb(II) were 70 ppm of initial concentration, 40 ml of solution volume, and 0.01 g of adsorbent amounts. As shown in these figures, the adsorption capacity of U(VI) or Pb(II) was rapidly increased, which can be due to the many accessibility of active sites on the adsorbents.

Results indicated that the uranium sorption reaches equilibrium at its maximum value in the initial 5 min. These results indicated that the synthesized magnetic nanostructures exhibit considerably shorter time to reach its maximum value than in previous reports. The sorption process was not changed by a further increase in the contact time. The equilibriums for Pb(II) adsorption on CoFe₂O₄ and CoFe₂O₄/MWCNTs were observed at approximately 120 and 90 min, respectively.

One of the most important parameters used to compare adsorption capability of synthesized adsorbents is studying their sorption isotherms. The sorption isotherms are usually calculated by simulating experimental results based on one of the existing models, such as Langmuir and Freundlich models. Figures 8, 9, and 10 show the sorption isotherms based on adsorption percentage, Langmuir isotherms, and Freundlich isotherms for adsorption of uranium and lead ions onto magnetite CoFe₂O₄ and CoFe₂O₄/MWCNTs nanostructures, respectively. Langmuir model is expressed based on the following equation:

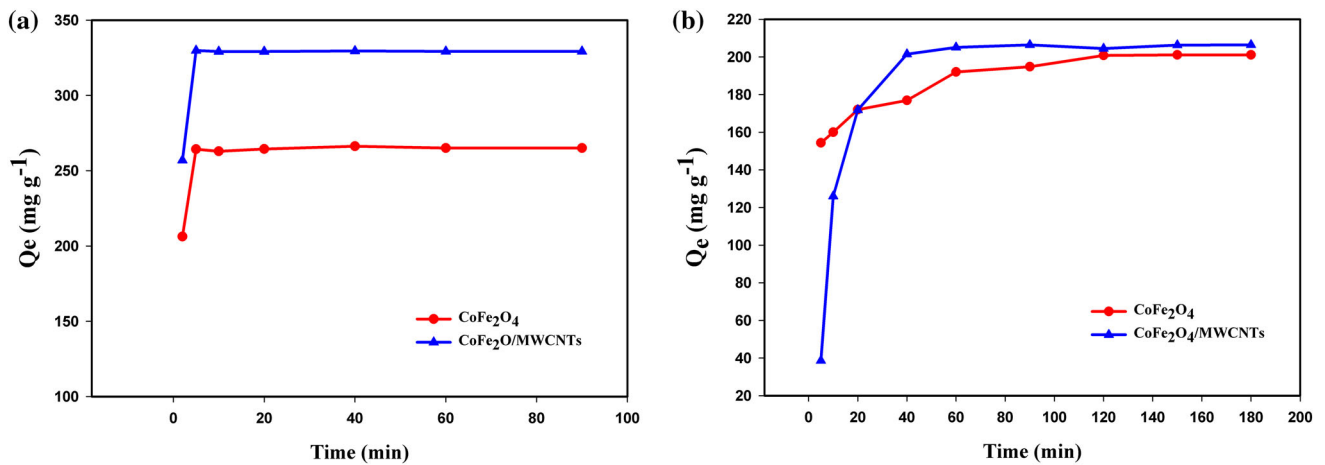


Fig. 7 Effect of contact time on **a** U(VI) adsorption, **b** Pb(II) adsorption by magnetite CoFe_2O_4 nanoparticles and $\text{CoFe}_2\text{O}_4/\text{MWCNTs}$ nanocomposites

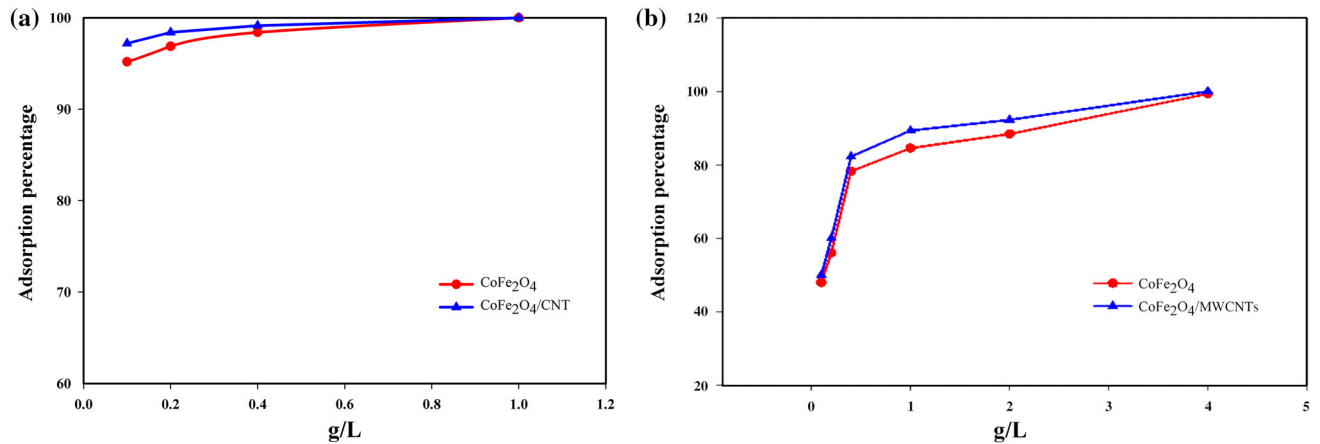


Fig. 8 Adsorption percentages for **a** U(VI) and **b** Pb(II) ions onto magnetite CoFe_2O_4 nanoparticles and $\text{CoFe}_2\text{O}_4/\text{MWCNTs}$ nanocomposites

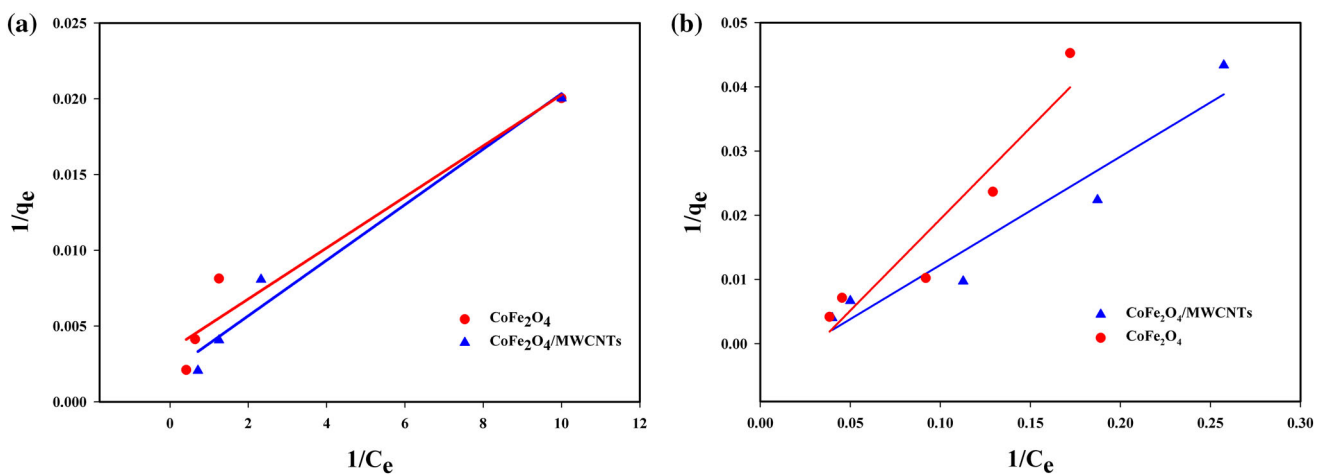


Fig. 9 Langmuir isotherm for adsorption of **a** U(VI), **b** Pb(II) on CoFe_2O_4 nanoparticles and $\text{CoFe}_2\text{O}_4/\text{MWCNTs}$ nanocomposites

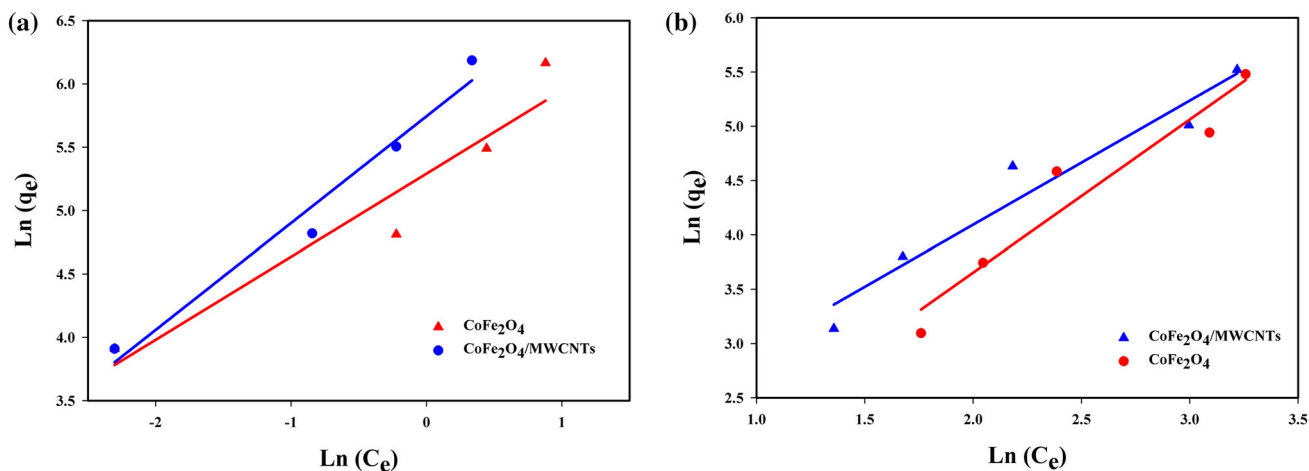


Fig. 10 Freundlich isotherm for adsorption of a U(VI), b Pb(II) on CoFe₂O₄ nanoparticles and CoFe₂O₄/MWCNTs nanocomposites

Table 3 Parameters of adsorption isotherms for the adsorption of U(VI) and Pb(II) on CoFe₂O₄ nanoparticles and CoFe₂O₄/MWCNTs nanocomposites

	CoFe ₂ O ₄		CoFe ₂ O ₄ /MWCNTs	
	U(VI)	Pb(II)	U(VI)	Pb(II)
Langmuir model				
Q _m (mg g ⁻¹)	294.12	109.89	500	217.39
K _L (l mg ⁻¹)	2	0.032	1.11	0.027
R ²	0.94	0.91	0.97	0.93
Freundlich model				
K _F (mg ^{1-1/n} l ^{1/n} g ⁻¹)	198.561	2.3	312.3	6.09
n	1.52	0.71	1.19	0.87
R ²	0.95	0.93	0.97	0.94

$$\frac{1}{q_e} = \frac{1}{q_m} + \frac{1}{K_L q_m} \cdot \frac{1}{C_e} \tag{3}$$

where q_e is the equilibrium adsorption uranium or lead ions in mg/g, C_e is the equilibrium concentration ions in mg/l, q_m is the maximum adsorption capacity in mg/g, and K_L is the Langmuir constant, which is related to the energy of adsorption.

Freundlich model:

$$\ln(q_e) = \ln(K_F) + \left(\frac{1}{n}\right) \ln(C_e) \tag{4}$$

where q_e is the amount of uranium or lead sorbed on the adsorbent in mg/g, C_e is the equilibrium concentration ions in mg/l, and K_F (mg¹⁻ⁿ lⁿ/g) and n are empirical constants that indicate the relative adsorption capacity and the adsorption intensity, respectively. Table 3 summarizes the Langmuir and Freundlich adsorption constants and the calculated regression coefficients (R^2). The Freundlich isotherm provided higher R^2 values than the Langmuir isotherm for the adsorption of Pb and U ions onto either adsorbent, indicating its better fit with the experimental data.

The maximum monolayer adsorption capacity (Q_{max}) of Pb(II) onto CoFe₂O₄ nanoparticles was calculated to be 109.89 mg g⁻¹, and the corresponding value for CoFe₂O₄/MWCNTs nanocomposites was 217.39 mg g⁻¹, which indicates the favorable effects of decorated MWCNT on the removal of Pb. The maximum adsorption capacities calculated from the Langmuir equation for U(VI) adsorption were 294.12 mg g⁻¹ for CoFe₂O₄ nanoparticles and 500 mg g⁻¹ for CoFe₂O₄/MWCNTs nanocomposites, which showed that the synthesized nanostructures present

Table 4 The maximum adsorption capacities Q (mg g⁻¹) of U(VI) on CoFe₂O₄ nanoparticles and CoFe₂O₄/MWCNTs nanocomposites and other adsorbents

Adsorbents	Adsorption capacity of U (mg g ⁻¹)	References
CoFe ₂ O ₄ /MWCNTs	212.7	[22]
Fe ₃ O ₄	85.35	[2]
Fe ₃ O ₄ -NH ₂	268.49	
Fe ₃ O ₄ /MWCNTs	24.28	[7]
Multiwalled carbon nanotubes (MWCNTs)	39.1	[42]
CoFe ₂ O ₄	294.12	Present work

higher adsorption capacities than those of previous works (Table 4) [8].

Conclusions

In this research, magnetite CoFe_2O_4 nanoparticle and $\text{CoFe}_2\text{O}_4/\text{MWCNTs}$ nanocomposite adsorbents with a high specific surface area, high adsorption capacity, and easily separated properties have been synthesized by the hydrothermal method for uranium and lead removal from aqueous solutions. The structural characteristics of synthesized nanostructures were confirmed by FT-IR, XRD, SEM, and BET analyses. The XRD pattern of synthesized magnetite CoFe_2O_4 nanoparticles indicates that the position and intensities of nearly all of the peaks are well matched to those of the other experimental results and the standard PDF cards for CoFe_2O_4 nanoparticles (JCPDS 22-1086 and JCPDS 79-1744). The SEM images indicate that the synthesized magnetic CoFe_2O_4 nanoparticles are composed of spherical nanoparticles, which have the average diameter of approximately 40 nm. Moreover, the average diameter of CoFe_2O_4 nanoparticles decorated on MWCNTs is approximately 34 nm. The estimated specific surface areas obtained by BET analysis were 113.4 and 186.1 $\text{m}^2 \text{g}^{-1}$ for CoFe_2O_4 and $\text{CoFe}_2\text{O}_4/\text{MWCNTs}$, respectively. The batch sorption technique was applied to investigate the adsorption properties of prepared nanocomposites. The adsorption capacities of uranium and lead onto CoFe_2O_4 nanoparticles and $\text{CoFe}_2\text{O}_4/\text{MWCNTs}$ nanocomposites were obtained as 294.12, 500, 109.89 and 217.39 mg g^{-1} , respectively. Several parameters, including pH, contact time, initial U(VI) concentration and solution volume, and adsorbent concentration, which influence the adsorption capacity were also investigated.

Acknowledgements The support from Shahid Beheshti University is gratefully acknowledged.

References

- Deng S, Ting YP (2005) Fungal biomass with grafted poly (acrylic acid) for enhancement of Cu (II) and Cd (II) biosorption. *Langmuir* 21(13):5940–5948
- Peng GW, Ding DX, Xiao FZ, Wang XL, Hun N, Wang YD et al (2014) Adsorption of uranium ions from aqueous solution by amine-group functionalized magnetic Fe_3O_4 nanoparticle. *J Radioanal Nucl Chem* 301(3):781–788
- Jamshidiyan M, Shirani AS, Alahyarizadeh G (2017) Solvothermal synthesis and characterization of magnetic Fe_3O_4 nanoparticle by different sodium salt sources. *Mater Sci Pol* 35(1):50–57
- Guerra DL, Leidens VL, Viana RR, Airolidi C (2010) Application of Brazilian kaolinite clay as adsorbent to removal of U (VI) from aqueous solution: kinetic and thermodynamic of cation–basic interactions. *J Solid State Chem* 183(5):1141–1149
- Um W, Serne RJ, Brown CF, Rod KA (2008) Uranium (VI) sorption on iron oxides in Hanford Site sediment: application of a surface complexation model. *Appl Geochem* 23(9):2649–2657
- Faghihian H, Rahi D, Mostajaboddavati M (2012) Study of natural radionuclides in Karun river region. *J Radioanal Nucl Chem* 292(2):711–717
- Zong P, Gou J (2014) Rapid and economical synthesis of magnetic multiwalled carbon nanotube/iron oxide composite and its application in preconcentration of U (VI). *J Mol Liq* 195:92–98
- Kurtio P, Auvinen A, Salonen L, Saha H, Pekkanen J, Mäkeläinen I et al (2002) Renal effects of uranium in drinking water. *Environ Health Perspect* 110(4):337
- Fu F, Wang Q (2011) Removal of heavy metal ions from wastewaters: a review. *J Environ Manag* 92(3):407–418
- Mehta D, Mazumdar S, Singh SK (2015) Magnetic adsorbents for the treatment of water/wastewater—a review. *J Water Process Eng* 7:244–265
- Mellah A, Chegrouche S, Barkat M (2006) The removal of uranium (VI) from aqueous solutions onto activated carbon: kinetic and thermodynamic investigations. *J Colloid Interface Sci* 296(2):434–441
- Bhatnagar A, Sillanpää M (2010) Utilization of agro-industrial and municipal waste materials as potential adsorbents for water treatment—a review. *Chem Eng J* 157(2):277–296
- Pala A, Tokat E (2002) Color removal from cotton textile industry wastewater in an activated sludge system with various additives. *Water Res* 36(11):2920–2925
- Szpyrkowicz L, Naumczyk J, Zilio-Grandi F (1995) Electrochemical treatment of tannery wastewater using TiPt and Ti/Pt/Ir electrodes. *Water Res* 29(2):517–524
- Bratskaya SY, Pestov AV, Yatluk YG, Avramenko VA (2009) Heavy metals removal by flocculation/precipitation using N-(2-carboxyethyl) chitosans. *Colloids Surf A* 339(1):140–144
- Farghali AA, Bahgat M, ElRouby WM, Khedr MH (2013) Decoration of multi-walled carbon nanotubes (MWCNTs) with different ferrite nanoparticles and its use as an adsorbent. *J Nanostruct Chem* 3(1):50
- Wang W, Li C, Yao J, Zhang B, Zhang Y, Liu J (2013) Rapid adsorption of neutral red from aqueous solutions by $\text{Zn}_3[\text{Co}(\text{CN})_6]_2 \cdot n\text{H}_2\text{O}$ nanospheres. *J Mol Liq* 184:10–16
- Zhang Y, Yan L, Xu W, Guo X, Cui L, Gao L et al (2014) Adsorption of Pb(II) and Hg(II) from aqueous solution using magnetic CoFe_2O_4 -reduced graphene oxide. *J Mol Liq* 191:177–182
- Fan FL, Qin Z, Bai J, Rong WD, Fan FY, Tian W et al (2012) Rapid removal of uranium from aqueous solutions using magnetic $\text{Fe}_3\text{O}_4/\text{SiO}_2$ composite particles. *J Environ Radioact* 106:40–46
- Xin X, Wei Q, Yang J, Yan L, Feng R, Chen G et al (2012) Highly efficient removal of heavy metal ions by amine-functionalized mesoporous Fe_3O_4 nanoparticles. *Chem Eng J* 184:132–140
- Zhao L, Zhang H, Xing Y, Song S, Yu S, Shi W et al (2008) Studies on the magnetism of cobalt ferrite nanocrystals synthesized by hydrothermal method. *J Solid State Chem* 181(2):245–252
- Tan L, Liu Q, Jing X, Liu J, Song D, Hu S et al (2015) Removal of uranium (VI) ions from aqueous solution by magnetic cobalt ferrite/multiwalled carbon nanotubes composites. *Chem Eng J* 273:307–315
- Baruwati B, Nadagouda MN, Varma RS (2008) Bulk synthesis of monodisperse ferrite nanoparticles at water–organic interfaces under conventional and microwave hydrothermal treatment and their surface functionalization. *J Phys Chem C* 112(47):18399–18404

24. Liu XM, Fu SY, Zhu LP (2007) High-yield synthesis and characterization of monodisperse sub-microsized CoFe_2O_4 octahedra. *J Solid State Chem* 180(2):461–466
25. Chen F, Liu R, Xiao S, Zhang C (2014) Solvothermal synthesis in ethylene glycol and adsorption property of magnetic Fe_3O_4 microspheres. *Mater Res Bull* 55:38–42
26. Nabiyoumi G, Julae M, Ghanbari D, Aliabadi PC, Safaie N (2015) Room temperature synthesis and magnetic property studies of Fe_3O_4 nanoparticles prepared by a simple precipitation method. *J Ind Eng Chem* 21:599–603
27. Majidi S, Zeinali Sehgri F, Farkhani SM, Soleymani Goloujeh M, Akbarzadeh A (2016) Current methods for synthesis of magnetic nanoparticles. *Artif Cells Nanomed Biotechnol* 44(2):722–734
28. Davarpanah SJ, Karimian R, Piri F (2015) Chemically synthesis and characterization of iron and nickel oxide nanoparticles for biomedicine. *J Appl Biotechnol Rep* 2(1):207–209
29. Song W, Liu M, Hu R, Tan X, Li J (2014) Water-soluble polyacrylamide coated- Fe_3O_4 magnetic composites for high-efficient enrichment of U (VI) from radioactive wastewater. *Chem Eng J* 246:268–276
30. Li C, Wei Y, Liivat A, Zhu Y, Zhu J (2013) Microwave-solvothermal synthesis of Fe_3O_4 magnetic nanoparticles. *Mater Lett* 107:23–26
31. Zhao Y, Li J, Zhao L, Zhang S, Huang Y, Wu X, Wang X (2014) Synthesis of amidoxime-functionalized $\text{Fe}_3\text{O}_4@/\text{SiO}_2$ core-shell magnetic microspheres for highly efficient sorption of U (VI). *Chem Eng J* 235:275–283
32. Ahmadpour A, Eftekhari N, Ayati A (2014) Performance of MWCNTs and a low-cost adsorbent for chromium (VI) ion removal. *J Nanostruct Chem* 4(4):171–178
33. Wang X, Chen C, Hu W, Ding A, Xu D, Zhou X (2005) Sorption of ^{243}Am (III) to multiwall carbon nanotubes. *Environ Sci Technol* 39(8):2856–2860
34. Chen CL, Wang XK, Nagatsu M (2009) Europium adsorption on multiwall carbon nanotube/iron oxide magnetic composite in the presence of polyacrylic acid. *Environ Sci Technol* 43(7):2362–2367
35. Yang S, Guo Z, Sheng G, Wang X (2012) Investigation of the sequestration mechanisms of Cd (II) and 1-naphthol on discharged multi-walled carbon nanotubes in aqueous environment. *Sci Total Environ* 420:214–221
36. Sundararajan M, Ghosh SK (2011) Designing novel materials through functionalization of carbon nanotubes for application in nuclear waste management: speciation of uranyl. *J Phys Chem A* 115(24):6732–6737
37. Shen YF, Tang J, Nie ZH, Wang YD, Ren Y, Zuo L (2009) Preparation and application of magnetic Fe_3O_4 nanoparticles for wastewater purification. *Sep Purif Technol* 68(3):312–319
38. Habibi MH, Parhizkar HJ (2014) FTIR and UV–vis diffuse reflectance spectroscopy studies of the wet chemical (WC) route synthesized nano-structure CoFe_2O_4 from CoCl_2 and FeCl_3 . *Spectrochim Acta Part A Mol Biomol Spectrosc* 127:102–106
39. Zhang S, Niu H, Cai Y, Zhao X, Shi Y (2010) Arsenite and arsenate adsorption on coprecipitated bimetal oxide magnetic nanomaterials: MnFe_2O_4 and CoFe_2O_4 . *Chem Eng J* 158(3):599–607
40. Vazquez-Olmos AR, Abatal M, Sato-Berru RY, Pedraza-Basulto GK, Garcia-Vazquez V, Sainz-Vidal A et al (2016) Mechano-synthesis of MFe_2O_4 (M = Co, Ni, and Zn) magnetic nanoparticles for Pb removal from aqueous solution. *J Nanomater* 2016. <https://doi.org/10.1155/2016/9182024>
41. Wei J, Zhang X, Liu Q, Li Z, Liu L, Wang J (2014) Magnetic separation of uranium by CoFe_2O_4 hollow spheres. *Chem Eng J* 241:228–234
42. Fafous II, Dawoud JN (2012) Uranium (VI) sorption by multi-walled carbon nanotubes from aqueous solution. *Appl Surf Sci* 259:433–440
43. Liu Y, Jiang W, Xu L, Yang X, Li F (2009) Decoration of carbon nanotubes with nearly monodisperse $\text{M}^{\text{II}}\text{Fe}_2\text{O}_4$ (MFe_2O_4 , M = Fe, Co, Ni) nanoparticles. *Mater Lett* 63(28):2526–2528
44. Jiang W, Liu Y, Li F, Chu J, Chen K (2010) Superparamagnetic cobalt-ferrite-modified carbon nanotubes using a facile method. *Mater Sci Eng B* 166(2):132–134
45. Li N, Zheng M, Chang X, Ji G, Lu H, Xue L et al (2011) Preparation of magnetic CoFe_2O_4 -functionalized graphene sheets via a facile hydrothermal method and their adsorption properties. *J Solid State Chem* 184(4):953–958
46. Wu H, Liu G, Wang X, Zhang J, Chen Y, Shi J et al (2011) Solvothermal synthesis of cobalt ferrite nanoparticles loaded on multiwalled carbon nanotubes for magnetic resonance imaging and drug delivery. *Acta Biomater* 7(9):3496–3504
47. Boobalan T, Suriyanarayanan N, Pavithradevi S (2013) Structural, magnetic and dielectric properties of nanocrystalline cobalt ferrite by wet hydroxyl chemical route. *Mater Sci Semicond Process* 16(6):1695–1700
48. Rana S, Philip J, Raj B (2010) Micelle based synthesis of cobalt ferrite nanoparticles and its characterization using fourier transform infrared transmission spectrometry and thermogravimetry. *Mater Chem Phys* 124(1):264–269
49. Bahgat M, Farghali AA, El Roubi WMA, Khedr MH (2011) Synthesis and modification of multi-walled carbon nano-tubes (MWCNTs) for water treatment applications. *J Anal Appl Pyrol* 92(2):307–313
50. Sing KS (1985) Reporting physisorption data for gas/solid systems with special reference to the determination of surface area and porosity (Recommendations 1984). *Pure Appl Chem* 57(4):603–619
51. Zhou L, Ji L, Ma PC, Shao Y, Zhang H, Gao W, Li Y (2014) Development of carbon nanotubes/ CoFe_2O_4 magnetic hybrid material for removal of tetrabromobisphenol A and Pb(II). *J Hazard Mater* 265:104–114
52. Wang F, Sun W, Pan W, Xu N (2015) Adsorption of sulfamethoxazole and 17β -estradiol by carbon nanotubes/ CoFe_2O_4 composites. *Chem Eng J* 274:17–29
53. Zhu L, Yuan LY, Xia LS, Wang L (2016) Incorporation of magnetism into the dihydroimidazole functionalized mesoporous silica for convenient U (VI) capture. *J Radioanal Nucl Chem* 308(2):447–458
54. Guo W, Nie C, Wang L, Li Z, Zhu L, Zhu L et al (2016) Easily prepared and stable functionalized magnetic ordered mesoporous silica for efficient uranium extraction. *Sci China Chem* 59(5):629–636